BULLETIN OF THE BRAZILIAN MATHEMATICAL SOCIETY

Bull Braz Math Soc, New Series 47(1), 187-200

ISSN: 1678-7544 (Print) / 1678-7714 (Online)

On second-order antidiffusive Lagrangian-remap schemes for multispecies kinematic flow models

Raimund Bürger, Christophe Chalons
and Luis Miguel Villada*

Abstract. This paper focuses on the numerical approximation of the solutions of multi-species kinematic flow models. These models are strongly coupled nonlinear first-order conservation laws with various applications like sedimentation of a polydisperse suspension in a viscous fluid, or traffic flow modeling. Since the eigenvalues and eigenvectors of the corresponding flux Jacobian matrix have no closed algebraic form, this is a challenging issue. A new class of simple schemes based on a Lagrangian-Eulerian decomposition (the so-called Lagrangian-remap (LR) schemes) was recently advanced in [4] for traffic flow models with nonnegative velocities, and extended to models of polydisperse sedimentation in [5]. These schemes are supported by a partial numerical analysis when one species is considered only, and turned out to be competitive in both accuracy and efficiency with several existing schemes. Since they are only first-order accurate, it is the purpose of this contribution to propose an extension to second-order accuracy using quite standard MUSCL and Runge-Kutta techniques. Numerical illustrations are proposed for both applications and involving eleven species (sedimentation) and nine species (traffic) respectively.

Keywords: system of conservation laws, Lagrangian-remap scheme, antidiffusive scheme, second-order scheme, polydisperse sedimentation, multiclass traffic model.

Mathematical subject classification: 35L65, 65M06, 65C99.

1 Introduction

This paper is concerned with the design of numerical methods for systems of strongly coupled nonlinear first-order conservation laws

$$\partial_t \Phi + \partial_x \boldsymbol{f}(\Phi) = \mathbf{0}, \quad x \in (0, L), \quad t > 0, \tag{1.1}$$

Received 16 March 2015.
*Corresponding author.

where $\Phi = (\phi_1, \ldots, \phi_N)^{\mathrm{T}}$ is the sought solution as a function of spatial position x and time t, $\boldsymbol{f}(\Phi) = (f_1(\Phi), \ldots, f_N(\Phi))^{\mathrm{T}}$ is a vector of flux density functions

$$f_i(\Phi) = \phi_i v_i(\Phi), \quad i = 1, \ldots, N, \tag{1.2}$$

and $v_i(\Phi)$ is the velocity of particle species i, which is assumed to be a given function of Φ. We will focus on applications to sedimentation of a polydisperse suspension and traffic flows where such models naturally appear.

The numerical approximation of (1.1)-(1.2) is a challenge since the eigenvalues and eigenvectors of $\mathcal{J}_{\boldsymbol{f}}(\Phi)$ are not available in closed form, so numerical schemes that rely on characteristic information become fairly involved (but are still competitive in efficiency [6, 9]). Alternatively, one can construct easy-to-implement numerical schemes for (1.1) by exploiting the concentration-times-velocity form (1.2) of the fluxes. These properties were first used in [7] to design simple difference schemes for (1.1)-(1.2).

In [4], one step Lagrangian-antidiffusive remap (L-AR) methods were applied to the multiclass Lighthill-Whitham-Richards (MCLWR) model for vehicular traffic which fall in the present framework. L-AR methods do not rely on spectral (characteristic) information and are as easy to implement as the schemes introduced in [7], but are more accurate and efficient. In [5] these schemes were extended to polydisperse sedimentation models. It is the goal of this paper to propose an extension of L-AR schemes introduced in [4, 5] to second order accuracy for approximating the solutions of equations (1.1)-(1.2).

To explain the main idea of L-AR schemes, consider the scalar continuity equation for a single species:

$$\partial_t \phi + \partial_x\big(\phi v(\phi)\big) = 0, \quad x \in (0, L), \quad t > 0. \tag{1.3}$$

We formally rewrite (1.3) as

$$\partial_t \phi + \phi \partial_x\big(v(\phi)\big) + v(\phi)\partial_x \phi = 0, \quad x \in (0, L), \quad t > 0. \tag{1.4}$$

L-AR schemes for (1.3) are based on splitting (1.4) into two different equations, which are solved successively for each time iteration. To advance the solution from time t to $t + \Delta t$, we first apply a Lagrangian method [10] to solve

$$\partial_t \phi + \phi \partial_x v(\phi) = 0, \tag{1.5}$$

and use this solution, evolved over a time interval of length Δt, as the initial condition for solving in a second step the transport equation

$$\partial_t \phi + v(\phi)\partial_x \phi = 0, \tag{1.6}$$

whose solution, again evolved over a time interval of length Δt, provides the sought approximate solution of (1.3) valid for time $t + \Delta t$. These steps will be identified as "Lagrangian" and "remap" steps, respectively, which explains why the schemes under study are addressed as "Lagrangian-remap" (LR) schemes. The specific idea behind "Lagrangian-antidiffusive remap" L-AR schemes is to solve (1.6) by recent antidiffusive techniques for transport equations [2, 3, 8], and thereby to increase the overall efficiency of the proposed splitting strategy, while keeping its simplicity. Importantly, these techniques are used and extended to our purpose in such a way that the resulting scheme (first step followed by second step) is conservative.

2 Models under consideration

2.1 Multiclass Lighthill-Whitham-Richards (MCLWR) traffic model

The multiclass Lighthill-Whitham-Richards traffic model, proposed by Benzoni-Gavage and Colombo [1] and Wong and Wong [16], is an extension of the well-known LWR kinematic traffic model for drivers having the same behavior to N classes of drivers, where different classes of drivers are assumed to have different preferential velocities. The MCLWR model leads to a system of equation in the form (1.1)-(1.2), where x is the horizontal distance and either $I = \mathbb{R}$ for an unbounded highway or $I = (0, L)$ for a traffic circle of length $L > 0$, t is the time, $\phi_i = \phi_i(x, t)$ is the local density of cars of class i, and $v_i(\phi)$ is the velocity of cars of class i, which is assumed to be a function of the total density $\phi := \phi_1 + \cdots + \phi_N$. We assume that for all i, $0 \le \phi_i \le \phi \le \phi_{\max}$, where $\phi_{\max}$ is a maximum density corresponding to a bumper-to-bumper situation, and that $v_i(\Phi) = v_i^{\max} V(\phi)$ for $i = 1, \ldots, N$, where $v_i^{\max}$ is the preferential velocity of class i corresponding to a free highway and $V(\phi)$ is a hindrance factor that takes into account drivers' attitude to reduce speed in presence of other cars. The function V is usually assumed to satisfy

$$V(0) = 1, \quad V'(\phi) \le 0 \quad \text{for } 0 \le \phi \le \phi_{\max}, \quad V(\phi_{\max}) = 0. \tag{2.1}$$

2.2 Polydisperse sedimentation model

Models of sedimentation of polydisperse suspensions of N small spherical particles suspended in a viscous fluid can be described in the form (1.1)-(1.2), where x denotes vertical distance, t is time, $\phi_i = \phi_i(x, t)$ is the local volume fraction of particles of species i having diameter d_i and density ϱ_i, where we assume $d_1 \ge d_2 \ge \cdots \ge d_N$. Batch sedimentation of a suspension of given

initial composition in a column of height L is then modeled by (1.1) under the specific assumption (1.2) along with the initial condition

$$\Phi(x,0) = \Phi_0(x), \quad x \in (0,L)$$

and zero-flux boundary conditions

$$f_i|_{x=0} = f_i|_{x=L} = 0, \quad i = 1,\dots,N,$$

where we assume that $\Phi_0 \in (L^1(0,L))^N$, and that Φ_0 takes values in the set $\mathcal{D}_{\phi_{\max}}$ of physically relevant concentration vectors defined by

$$\mathcal{D}_{\phi_{\max}} := \left\{(\phi_1,\dots,\phi_N)^{\mathrm{T}} \in \mathbb{R}^N : \phi_1 \geq 0,\dots,\phi_N \geq 0,\ \phi_1 + \cdots + \phi_N \leq \phi_{\max}\right\},$$

where $\phi_{\max}$ is a maximum total solids concentration. The MLB model of polydisperse sedimentation [11, 12] is based on the following velocity function for particles of species i (having size d_i and density ϱ_i):

$$\begin{aligned} v_i(\Phi) &= v_i^{\mathrm{MLB}}(\Phi) \\ &= \mu V(\phi)\left[\delta_i(\bar{\varrho}_i - \bar{\boldsymbol{\varrho}}^{\mathrm{T}}\Phi) - \sum_{l=1}^{N}\delta_l\phi_l(\bar{\varrho}_l - \bar{\boldsymbol{\varrho}}^{\mathrm{T}}\Phi)\right], \quad i = 1,\dots,N. \end{aligned} \tag{2.2}$$

Here $\mu = gd_1^2/(18\mu_{\mathrm{f}})$, where g denotes the acceleration of gravity, μ_{f} is the viscosity of the fluid, $\delta_i := d_i^2/d_1^2$, $\bar{\varrho}_i := \varrho_i - \varrho_{\mathrm{f}}$, where ϱ_{f} is the density of the fluid, $\bar{\boldsymbol{\varrho}} := (\bar{\varrho}_1,\dots,\bar{\varrho}_N)^{\mathrm{T}}$, and $V(\phi)$ is a so-called hindered settling factor, which is a given function $V = V(\phi)$ of the total solids volume fraction $\phi := \phi_1 + \cdots + \phi_N$ that is assumed to satisfy (2.1). For equal-density particles, we have $\varrho_i =: \varrho_{\mathrm{s}}$ for $i = 1,\dots,N$. We define $\boldsymbol{\delta} := (\delta_1,\delta_2,\dots,\delta_N)^{\mathrm{T}}$, $\delta_1 = 1$. Then (2.2) reduces to

$$v_i(\Phi) = \mu(\varrho_{\mathrm{s}} - \varrho_{\mathrm{f}})V(\phi)(1-\phi)(\delta_i - \boldsymbol{\delta}^{\mathrm{T}}\Phi). \tag{2.3}$$

Since $\phi_{\max} \leq 1$, the function $\phi \mapsto V(\phi)(1-\phi)$ satisfies (2.1), we may absorb $(\varrho_{\mathrm{s}} - \varrho_{\mathrm{f}})$ into the constant μ and the factor $(1-\phi)$ into $V(\phi)$ to obtain the following simplified equation instead of (2.3):

$$v_i(\Phi) = \mu V(\phi)(\delta_i - \boldsymbol{\delta}^{\mathrm{T}}\Phi). \tag{2.4}$$

A common expression for $V(\phi)$ appearing in (2.4) is the following Richardson-Zaki [13] formula, where $n_{\mathrm{RZ}} \geq 2$ is a material specific exponent:

$$V(\phi) = \begin{cases} (1-\phi)^{n_{\mathrm{RZ}}} & \text{for } 0 \leq \phi \leq \phi_{\max}, \\ 0 & \text{for } \phi > \phi_{\max}. \end{cases}$$

3 Lagrangian-Antidiffusive Remap (L-AR) schemes

3.1 Spatial discretization

If $\Delta x = L/M$ denotes a spatial meshsize, $x_j = (j-1/2)\Delta x$ for $j = 1, \ldots, M$, $\Delta t > 0$ is a time step, $t^n := n\Delta t$, and ϕ_{ij}^n denotes the approximate cell average of ϕ_i on the cell $[x_{j-1/2}, x_{j+1/2}] \times [t^n, t^{n+1})$. The ratio $\lambda := \Delta t/\Delta x$ must satisfy a certain CFL condition that will be specified below. We denote by $v_{j+1/2}^n$ an approximate value of $v(\phi)$ at the interface point $x = x_{j+1/2}$ at time t^n. We focus first on the discretization of the scalar equation (1.3).

3.2 Lagrangian step for the scalar model ($N = 1$)

Defining $\tau := 1/\phi$, we obtain from (1.5) the conservation of mass equation in Lagrangian coordinates

$$\phi \partial_t \tau - \partial_x v = 0. \tag{3.1}$$

In other words, solving (1.5), or equivalently (3.1), means solving the original equation (1.3) on a moving referential mesh with velocity v. Assume now that $\boldsymbol{\phi}^n = (\phi_1^n, \ldots, \phi_M^n)^{\mathrm{T}}$ is an approximate solution of (1.3) at time $t = t^n$ and used as the initial condition for (3.1). Then a numerical solution $\boldsymbol{\phi}^{n+1,-}$ of (3.1) at time Δt can be naturally computed by

$$\phi_j^{n+1,-}\left[\Delta x + \left(v_{j+1/2}^n - v_{j-1/2}^n\right)\Delta t\right] = \phi_j^n \Delta x, \quad j = 1, \ldots, M. \tag{3.2}$$

In fact, (3.2) states that the initial mass in the cell $[x_{j-1/2}, x_{j+1/2}]$ at time t^n (the right-hand side) equals the mass in the modified cell $[\bar{x}_{j-1/2}, \bar{x}_{j+1/2}]$ at time Δt (the left-hand side), where $\bar{x}_{j+1/2} = x_{j+1/2} + v_{j+1/2}^n \Delta t$, are the new interface positions. A natural choice for the velocity values in the interface points is

$$v_{j+1/2}^n = \begin{cases} v(\phi_j^n) & \text{if } (v(\phi_{j+1}^n) - v(\phi_j^n))(\phi_{j+1}^n - \phi_j^n) > 0, \\ v(\phi_{j+1}^n) & \text{if } (v(\phi_{j+1}^n) - v(\phi_j^n))(\phi_{j+1}^n - \phi_j^n) \le 0, \end{cases} \tag{3.3}$$

which takes into account the possible change of sign of $v'(\phi)$.

3.3 Remap step: antidiffusive scheme for the scalar model ($N = 1$)

After the Lagrangian step, the new values $\phi_j^{n+1,-}$ represent approximate values of the density on a moved mesh with new cells $[\bar{x}_{j-1/2}, \bar{x}_{j+1/2}]$. To avoid dealing with moving meshes, a so-called remap step is necessary to define the new

approximations ϕ_j^{n+1} on the uniform mesh with cells $[x_{j-1/2}, x_{j+1/2}]$. This step amounts to "averaging" the density values at time Δt on the cells $[x_{j-1/2}, x_{j+1/2}]$. This average step can equivalently be reformulated by using the solution of the transport equation (1.6) with initial data defined by $\phi_j^{n+1,-}$ on each cell $[x_{j-1/2}, x_{j+1/2}]$, i.e., we consider a numerical scheme in the form

$$\phi_j^{n+1} = \phi_j^{n+1,-} - \bar{V}_j^n \lambda \big(\phi_{j+1/2}^{n+1,-} - \phi_{j-1/2}^{n+1,-}\big), \quad j = 1, \ldots, M. \tag{3.4}$$

Here $\bar{V}_j^n$ is a velocity value, defined in terms of available density values, which will be chosen in such a way that the complete scheme (3.2), (3.4) is conservative with respect to (1.3). The quantities $\phi_{j+1/2}^{n+1,-}$, $j = 1, \ldots, M$, are numerical fluxes associated with the cell interfaces $x_{j-1/2}$ and will be chosen in such a way that the scheme (3.4) has certain stability and consistency properties.

There are different ways to define the quantities $\phi_{j+1/2}^{n+1,-}$; see [2, 3, 8] and [4, Section 4.2] for non-negative velocities, but we here proceed as in [4] and consider only the so-called N-Bee method described in [2], which is well-defined when velocities have variable signs and was shown to give the best results in [4]. This scheme corresponds to the choice

$$\phi_{j+1/2}^{n+1,-} = \begin{cases} \phi_{j+1/2}^{\mathrm{L}} := \phi_j^{n+1,-} \\ \qquad + \dfrac{1-\bar{\lambda}_j}{2} \varphi^{\mathrm{NB}}(r_j, \bar{\lambda}_j)\big(\phi_{j+1}^{n+1,-} - \phi_j^{n+1,-}\big) \\ \qquad\qquad \text{if } \bar{V}_j > 0 \text{ and } \bar{V}_{j+1} > 0, \\ \phi_{j+1/2}^{\mathrm{R}} := \phi_{j+1}^{n+1,-} \\ \qquad + \dfrac{1-|\bar{\lambda}_{j+1}|}{2} \varphi^{\mathrm{NB}}(r_{j+1}^-, |\bar{\lambda}_{j+1}|)\big(\phi_j^{n+1,-} - \phi_{j+1}^{n+1,-}\big) \\ \qquad\qquad \text{if } \bar{V}_j < 0 \text{ and } \bar{V}_{j+1} < 0, \\ \dfrac{\phi_{j+1}^{n+1,-} + \phi_j^{n+1,-}}{2} \qquad \text{if } \bar{V}_j \cdot \bar{V}_{j+1} < 0, \end{cases} \tag{3.5}$$

where $\bar{\lambda}_j = \lambda \bar{V}_j = \max(v_{j+1/2}, v_{j-1/2})$ and

$$r_j := \frac{\phi_j^{n+1,-} - \phi_{j-1}^{n+1,-}}{\phi_{j+1}^{n+1,-} - \phi_j^{n+1,-}}, \quad r_j^- := \frac{\phi_{j+1}^{n+1,-} - \phi_j^{n+1,-}}{\phi_j^{n+1,-} - \phi_{j-1}^{n+1,-}} = \frac{1}{r_j}.$$

The limiter function is defined as

$$\varphi^{\mathrm{NB}}(r, \bar{\lambda}) := \max\left\{0, \min\left\{1, \frac{2r}{\bar{\lambda}}\right\}, \min\left\{r, \frac{2}{1-\bar{\lambda}}\right\}\right\}.$$

3.4 Lagrangian-antidiffusive remap (L-AR) schemes for the scalar model ($N = 1$)

It was shown in [4] and [5] that the two steps (3.2) followed by (3.4) actually define a conservative scheme of the form

$$\phi_j^{n+1} = \phi_j^n - \lambda\big(F_{j+1/2}^n - F_{j-1/2}^n\big), \quad j = 1, \ldots, M. \tag{3.6}$$

where the corresponding numerical fluxes $F_{j+1/2}^n$ are computed as follow

$$F_{j+1/2}^n := \phi_{j+1/2}^{\mathrm{L}} \max\big\{0, v_{j+1/2}^n\big\} + \phi_{j+1/2}^{\mathrm{R}} \min\big\{0, v_{j+1/2}^n\big\}. \tag{3.7}$$

In other words, L-AR schemes can be implemented in a very simple manner in the following three steps

1. Compute $v_{j+1/2}^n$ according to (3.3) for $j = 0, \ldots, M$.
2. Compute $\boldsymbol{\phi}^{n+1,-}$ by the Lagrangian step (3.2).
3. Calculate the intermediate fluxes $\phi_{j+1/2}^{\mathrm{L}}$ and $\phi_{j+1/2}^{\mathrm{R}}$, $j = 0, \ldots, M$, by the NBee scheme (3.5), and apply (3.6)-(3.7).

3.5 Definition of L-AR schemes for $N > 1$

In order to define the L-AR schemes in the system case $N > 1$, we first naturally propose to define the intermediate velocities $v_{i,j+1/2}^n$, $i = 1, \ldots, N$, by applying (3.3) in a component-wise manner, giving rise to

$$v_{i,j+1/2}^n = \begin{cases} v_i(\Phi_j^n) & \text{if } (v_i(\Phi_{j+1}^n) - v_i(\Phi_j^n))(\phi_{j+1}^n - \phi_j^n) > 0, \\ v_i(\Phi_{j+1}^n) & \text{if } (v_i(\Phi_{j+1}^n) - v_i(\Phi_j^n))(\phi_{j+1}^n - \phi_j^n) \le 0, \end{cases} \quad i = 1, \ldots, N. \tag{3.8}$$

Based on (3.8), Lagrangian values $\phi_{i,j}^{n+1,-}$ are computed by considering (3.2) for each component, i.e.,

$$\phi_{i,j}^{n+1,-}\big[\Delta x + \big(v_{i,j+1/2}^n - v_{i,j-1/2}^n\big)\Delta t\big] = \phi_{ij}^n \Delta x, \quad i = 1, \ldots, N. \tag{3.9}$$

Finally, the numerical fluxes are given by

$$F_{i,j+1/2}^n := \phi_{i,j+1/2}^{\mathrm{L}} \max\big\{v_{i,j+1/2}^n, 0\big\} + \phi_{i,j+1/2}^{\mathrm{R}} \min\big\{v_{i,j+1/2}^n, 0\big\}, \quad i = 1, \ldots, N, \tag{3.10}$$

where $\phi_{i,j+1/2}^{\mathrm{L}}$ and $\phi_{i,j+1/2}^{\mathrm{R}}$ are computed according to (3.5) in each component. Thus, we refer to the *L-NBee scheme* for $N > 1$ as the numerical scheme (3.6) applied in a component-wise manner, with intermediate velocities (3.8), Lagrangian values $\phi_{i,j}^{n+1,-}$ as in (3.9), and numerical fluxes (3.10).

4 Extension to second-order accuracy in space and time

4.1 Second-order accuracy in space.

A standard device to upgrade a conservative difference scheme to second-order accuracy in space is MUSCL-type variable extrapolation [14, 15]. To implement it, we approximate $\phi(x, t^n)$ by a piecewise linear numerical solution in each cell, i.e., $\hat{\phi}_j(x, t^n) = \phi_j^n + \sigma_j^n(x - x_j)$, where the slopes σ_j^n are calculated via the standard minmod function, i.e.,

$$\sigma_j^n = \frac{1}{\Delta x}\operatorname{minmod}\big(\phi_j^n - \phi_{j-1}^n, \phi_{j+1}^n - \phi_j^n\big), \quad \text{where}$$
$$\operatorname{minmod}(a, b) = \begin{cases} \operatorname{sgn}(a)\min\{|a|, |b|\} & \text{if } \operatorname{sgn} a = \operatorname{sgn} b, \\ 0 & \text{otherwise.} \end{cases}$$

This extrapolation enables one to define left and right values defined by

$$\begin{aligned} \phi_{j+1/2,\mathrm{L}}^n &:= \hat{\phi}_j^n\left(x_j + \frac{\Delta x}{2}\right), \quad v_{j+1/2}^{\mathrm{L}} := v\big(\phi_{j+1/2,\mathrm{L}}^n\big), \\ \phi_{j+1/2,\mathrm{R}}^n &:= \hat{\phi}_{j+1}\left(x_{j+1} - \frac{\Delta x}{2}\right), \quad v_{j+1/2}^{\mathrm{R}} := v\big(\phi_{j+1/2,\mathrm{R}}^n\big), \\ & \qquad\qquad\qquad\qquad j = 1, \ldots, M. \end{aligned} \tag{4.1}$$

Equations (4.1) can be applied in a component-wise manner. Then for $N > 1$ we define intermediate velocities according to the formula

$$v_{i,j+1/2}^n = \begin{cases} v_{i,j+1/2}^{\mathrm{L}} & \text{if } (v_{i,j+1/2}^{\mathrm{R}} - v_{i,j+1/2}^{\mathrm{L}})(\phi_{j+1/2,\mathrm{R}}^n - \phi_{j+1/2,\mathrm{L}}^n) > 0, \\ v_{i,j+1/2}^{\mathrm{R}} & \text{if } (v_{i,j+1/2}^{\mathrm{R}} - v_{i,j+1/2}^{\mathrm{L}})(\phi_{j+1/2,\mathrm{R}}^n - \phi_{j+1/2,\mathrm{L}}^n) \le 0. \end{cases} \tag{4.2}$$

After that, Lagrangian values $\phi_{i,j}^{n+1,-}$ are computed as in (3.9) with $v_{i,j+1/2}^n$ as in (4.2). Next we compute $\phi_{i,j+1/2}^{\mathrm{L}}$ and $\phi_{i,j+1/2}^{\mathrm{R}}$ as in (3.5) with left and right values $j + 1/2, L$ and $j + 1/2, R$ instead of $j, j + 1$. Finally the numerical fluxes (3.10) are computing as

$$\begin{aligned} F_{i,j+1/2}^n := \phi_{i,j+1/2}^{\mathrm{L}} \max\big\{v_{i,j+1/2}^n, 0\big\} + \phi_{i,j+1/2}^{\mathrm{R}} \min\big\{v_{i,j+1/2}^n, 0\big\}, \\ i = 1, \ldots, N. \end{aligned} \tag{4.3}$$

4.2 Second-order accuracy in time

To obtain second-order accuracy in time, we propose to use a Runge-Kutta method that consists in writing the vector form of (3.6) component-wise with

(4.3) in the form $\Phi^{n+1} = \Phi^n + \lambda L^\lambda(\Phi^n)$ and replace it by the formula

$$\begin{cases} \Phi^{(1)} = \Phi^n + \lambda L^\lambda(\Phi^n) \\ \Phi^{n+1} = \dfrac{1}{2}(\Phi^n + \Phi^{(1)}) + \dfrac{\lambda}{2} L^{\lambda/2}(\Phi^{(1)}). \end{cases} \tag{4.4}$$

Here, $L^{\lambda/2}(\Phi^{(1)})$ means that $\phi^{\mathrm{L}}_{i,j+1/2}$ and $\phi^{\mathrm{R}}_{i,j+1/2}$ are computed according to (3.5) in each component using $\lambda/2$ instead of λ. A similar technique is used in [17].

From now on, we address as L-NBee-O2 scheme the numerical scheme (4.4) applied in a component-wise manner with intermediate velocities (4.2), Lagrangian values $\phi^{n+1,-}_{i,j}$ as in (3.9), and numerical fluxes (4.3).

5 Numerical examples

In the subsequent two examples, we solve system (1.1) numerically for $0 \le t \le T$ and $0 \le x \le L$ and start in each case with an initial condition, i.e., $\Phi_0(x) = \Phi^0 \in \mathcal{D}_{\phi_{\max}}$ for $x \in [0, L]$. We compare the numerical results obtained by the L-NBee and L-NBee-O2 schemes with those obtained by a first-order scheme, namely Scheme 4 of [7], and a second-order scheme, namely Scheme 10 of [7]. For each model, the interval $[0, 1]$ of normalized length x/L is subdivided into M subintervals of equal length Δx. For each iteration, Δt is determined by the following formula:

$$\Delta t = \frac{\Delta x}{2}\Big(\max_{i=1,\dots,N} \max_{\Phi \in \mathcal{D}_{\phi_{\max}}} |v_i(\Phi)|\Big)^{-1}.$$

Reference solutions to compute approximate errors are computed by the WENO-SPEC-INT scheme introduced in [6] with a fine mesh made of $M_{\mathrm{ref}} = 12800$ cells. Total approximate L^1 errors at different times for each scheme are computed as follows. Let us denote by $(\phi^M_{j,i}(t))_{j=1}^M$ and $(\phi^{\mathrm{ref}}_{l,i}(t))_{l=1}^{M_{\mathrm{ref}}}$ the numerical solution for the i-th component at time t calculated with M and M_{ref} cells, respectively. We use cubic interpolation from the reference grid to the M cells grid to compute $\widetilde{\phi}^{\mathrm{ref}}_{j,i}(t)$ for $j = 1, \dots, M$. We calculate the approximate L^1 error in species i by

$$e_i(t) := \frac{1}{M}\sum_{j=1}^{M} \big|\widetilde{\phi}^{\mathrm{ref}}_{j,i}(t) - \phi^M_{j,i}(t)\big|, \quad i = 1, \dots, N.$$

The total approximate L^1 error at time t is defined as $e_{\mathrm{tot}}(t) := e_1(t) + \cdots + e_N(t)$.

5.1 Example 1 (MLB model $N = 11$)

We consider the classical test [5, 6, 7] of a settling of a suspension of $N = 11$ species in a column of (unnormalized) height $L = 0.935$ m, the initial concentrations ϕ_i^0, diameters D_i, and normalized diameters $d_i = D_i/D_1$ given in Table 1, the maximum total concentration $\phi_{\max} = 0.641$.

i	1	2	3	4	5	6	7	8	9	10	11
$\phi_i^0[10^{-3}]$	0.435	3.747	14.420	32.603	47.912	47.762	32.663	15.104	4.511	0.783	0.060
$D_i[10^{-5}]$	8.769	8.345	7.921	7.497	7.073	6.649	6.225	5.801	5.377	4.953	4.529
d_i	1.000	0.952	0.903	0.855	0.807	0.758	0.710	0.662	0.613	0.565	0.516

Table 1: Example 1 (MLB model, $N = 11$): initial concentrations ϕ_i^0, real and normalized particles sizes D_i and d_i.

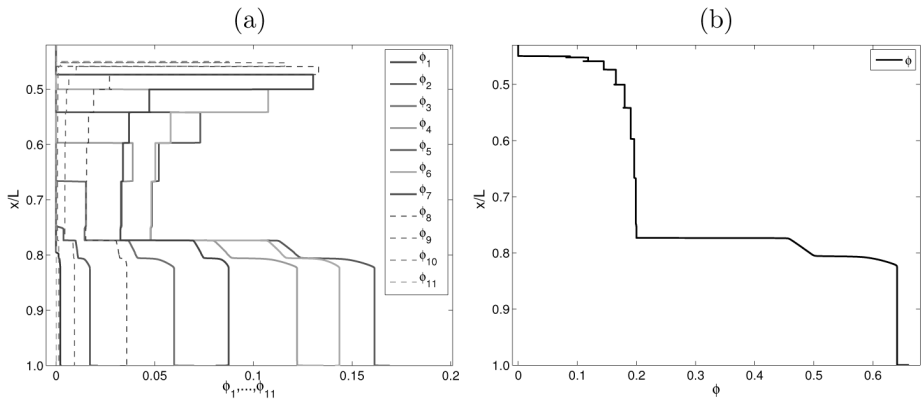

Figure 1: Example 1 (MLB model, $N = 11$): (a) numerical solution with L-NBee-O2 scheme at simulated time $T = 230$ s with $\Delta x = 1/6400$, (b) total concentration.

In Figures 1 (a) and (b) we display the numerical solution at time $T = 230$s obtained with L-NBee-O2 scheme with $\Delta x = 1/6400$. We see that the scheme capture the transient dynamics of the settling process. For this discretization level, the shocks and rarefaction waves are adequately approximated by this scheme in both each species and total concentration.

In Figures 2 (a), (b) and (c) we display details of the numerical solution with a discretization size $\Delta x = 1/800$ only for species ϕ_1, ϕ_5 and ϕ_7, comparing the results produced by schemes L-NBee-O2, L-NBee and Scheme 10 with the reference solution. Shock waves are approximated adequately by L-NBee-

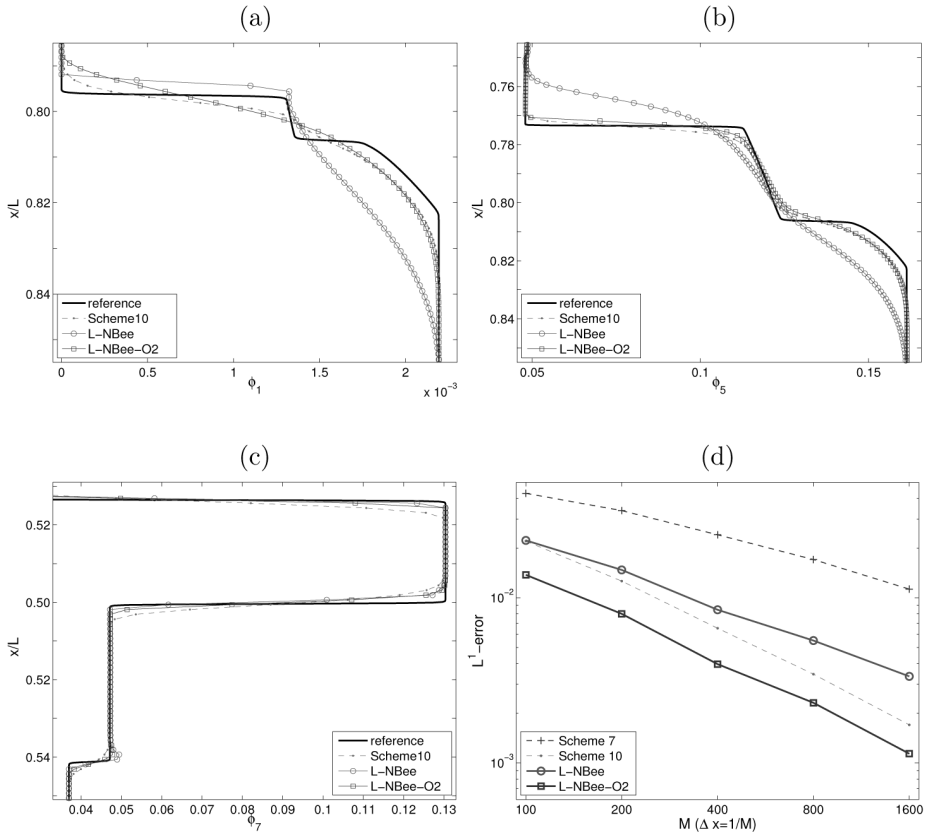

Figure 2: Example 1 (MLB model, $N = 11$): (a, b, c) details of the numerical solution for different schemes with $\Delta x = 1/800$ only for species ϕ_1, ϕ_5 and ϕ_7, compared with the reference solution, (d) total approximate L^1-error versus Δx for different values of M.

O2 scheme and the approximation is better than that of the L-NBee scheme in the rarefaction waves, and is similar to the approximation of the second-order Scheme 10. In Figure 2 (d) we display L^1-errors with respect to different levels of discretization $M = 100, 200, 400, 800, 1600$. We observe that errors for L-NBee-O2 are smaller than for L-NBee and Scheme 10, in particular we observe that the slope of the interpolation curve in L-NBee-O2 scheme is comparable with respect to second order Scheme 10 curve.

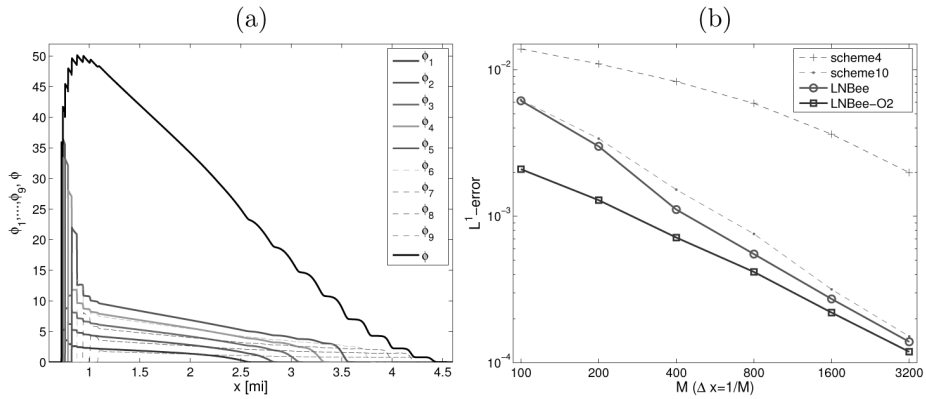

Figure 3: Example 2 (MCLWR model, $N = 9$): (a) numerical solution by L-NBee-O2 scheme at $T = 0.028$h with $\Delta x = 1/3200$, (b) total approximate L^1-error versus Δx for different values of M.

5.2 Example 2

We consider the MCLWR model (1.1) along with $N = 9$ and hindrance function $V(\phi) = \exp(-(\phi/\phi^*)^2/2)$ with $\phi^* = 50$[cars/mi] and the numerical test proposed in [16], where $\boldsymbol{\phi}(x, 0) = \boldsymbol{\phi}_0(x)$ describes an isolated platoon and $v_i^{\max} = (52.5 + 7.5i)$ mi/h, $i = 1, \ldots, 9$. We consider a road of length $L = 5$ mi, i.e. we set $I := [0, 5]$ and set $\boldsymbol{\Phi}_0(x) = 0.04p(x)\phi_0(1, 2, 3, 4, 5, 4, 3, 2, 1)^{\mathrm{T}}$, where

$$p(x) = \begin{cases} 10x & \text{for } 0 < x \le 0.1, \quad 1 \quad \text{for } 0.1 < x \le 0.9, \\ -10(x-1) & \text{for } 0.9 < x \le 1, \quad 0 \quad \text{otherwise.} \end{cases}$$

We set $\phi_0 = 100$ cars/mi $> \phi^*$, which leads to a congested regime.

In Figure 3 (a) we display the numerical solution obtained with L-NBee-O2 scheme at time $T = 0.028$h, the traffic phenomenon is represented adequately by this scheme. In Figure 3 (b) we display L^1-errors versus Δx. As in Example 1, we observe that errors for the L-NBee-O2 scheme are smaller than for the L-NBee scheme and Scheme 10.

6 Conclusion

We have extended the L-NBee schemes proposed in [4, 5] to second-order accuracy by using quite standard MUSCL and Runge-Kutta techniques. The

proposed numerical scheme addressed as L-NBee-O2 turns out to be competitive with respect to second-order schemes in the literature, which is especially interesting for large values of N.

Acknowledgements. RB is supported by Fondecyt project 1130154; BASAL project CMM, Universidad de Chile and Centro de Investigación en Ingeniería Matemática (CI^{2}MA), Universidad de Concepción; Conicyt project Anillo ACT-1118 (ANANUM); Red Doctoral REDOC.CTA, MINEDUC project UCO1202; and CRHIAM, project CONICYT/FONDAP/15130015. LMV is supported by Fondecyt project 11140708.

References

[1] S. Benzoni-Gavage and R.M. Colombo. *An n-populations model for traffic flow.* Eur. J. Appl. Math., **14** (2003), 587–612.

[2] O. Bokanowski and H. Zidani. *Anti-dissipative schemes for advection and application to Hamilton-Jacobi-Bellman equations*. J. Sci. Comput., **30** (2007), 1–33.

[3] F. Bouchut. *An anti-diffusive entropy scheme for monotone scalar conservation laws*. J. Sci. Comput., **21** (2004), 1–30.

[4] R. Bürger, C. Chalons and L.M. Villada. *Anti-diffusive and random-sampling Lagrangian-remap schemes for the multi-class Lighthill-Whitham-Richards traffic model*. SIAM J. Sci. Comput., **35** (2013), B1341–B1368.

[5] R. Bürger, C. Chalons and L.M. Villada. *Lagrangian-remap schemes for models of polydisperse sedimentation*, to appear in Num. Meth. PDEs.

[6] R. Bürger, R. Donat, P. Mulet and C.A. Vega. *On the implementation of WENO schemes for a class of polydisperse sedimentation models*. J. Comput. Phys., **230** (2011), 2322–2344.

[7] R. Bürger, A. García, K.H. Karlsen and J.D. Towers. *A family of numerical schemes for kinematic flows with discontinuous flux*. J. Eng. Math., **60** (2008), 387–425.

[8] B. Després and F. Lagoutière. *Contact discontinuity capturing schemes for linear advection and compressible gas dynamics*. J. Sci. Comput., **16** (2001), 479–524.

[9] R. Donat and P. Mulet. *Characteristic-based schemes for multi-class Lighthill-Whitham-Richards traffic models*. J. Sci. Comput., **37** (2008), 233–250.

[10] E. Godlewski and P.-A. Raviart. *Numerical Approximation of Hyperbolic Systems of Conservation Laws*. Springer Verlag, New York (1996).

[11] M.S. Lockett and K.S. Bassoon. *Sedimentation of binary particle mixtures*. Powder Technol., **24** (1979), 1–7.

[12] J.H. Masliyah. *Hindered settling in a multiple-species particle system*. Chem. Engrg. Sci., **34** (1979), 1166–1168.

[13] J.F. Richardson and W.N. Zaki. *Sedimentation and fluidization: Part I*. Trans. Inst. Chem. Eng. (London), **32** (1954), 35–53.

[14] B. van Leer. *Towards the ultimate conservative difference scheme. V. A second-order sequel to Godunov's method*. J. Comput. Phys., **32** (1979), 101–136.

[15] B. van Leer. *On the relation between the upwind-differencing schemes of Godunov, Engquist-Osher and Roe.* SIAM J. Sci. Statist. Comput., **5** (1984), 1–20.

[16] G.C.K. Wong and S.C. Wong. *A multi-class traffic flow model – an extension of LWR model with heterogeneous drivers.* Transp. Res. A, **36** (2002), 827–841.

[17] Z. Xu and C-W. Shu. *Anti-diffusive flux corrections for high order finite difference WENO schemes*. J. Comput. Phys. **205**(2) (2005), 458–485.

Raimund Bürger
CI^{2}MA and Departamento de Ingeniería Matemática
Facultad de Ciencias Físicas y Matemáticas
Universidad de Concepción
Casilla 160-C, Concepción
CHILE

E-mail: rburger@ing-mat.udec.cl

Christophe Chalons
Laboratoire de Mathématiques de Versailles
Université de Versailles Saint-Quentin-en-Yvelines
CNRS
Université Paris-Saclay
78035 Versailles
FRANCE

E-mail: christophe.chalons@uvsq.fr

Luis Miguel Villada
GIMNAP-Departamento de Matemáticas
Universidad del Bío-Bío
Casilla 5-C, Concepción
CHILE

and

CI2MA, Universidad de Concepción
Casilla 160-C, Concepción
CHILE

E-mail: lvillada@ubiobio.cl